

5-1-2010

An Experimental Investigation on Viscoelastic Behavior in Tunable

Hao-Han Hsu

Purdue University - Main Campus, hsub@purdue.edu

Dimitrios Peroulis

Birck Nanotechnology Center and School of Electrical and Computer Engineering, Purdue University, dperouli@purdue.edu

Follow this and additional works at: <http://docs.lib.purdue.edu/prism>



Part of the [Nanoscience and Nanotechnology Commons](#)

Hsu, Hao-Han and Peroulis, Dimitrios, "An Experimental Investigation on Viscoelastic Behavior in Tunable" (2010). *PRISM: NNSA Center for Prediction of Reliability, Integrity and Survivability of Microsystems*. Paper 46.
<http://docs.lib.purdue.edu/prism/46>

This document has been made available through Purdue e-Pubs, a service of the Purdue University Libraries. Please contact epubs@purdue.edu for additional information.

An Experimental Investigation on Viscoelastic Behavior in Tunable Planar RF-MEMS Resonators

Hao-Han Hsu and Dimitrios Peroulis

School of Electrical and Computer Engineering, Birck Nanotechnology Center,
Purdue University, West Lafayette, IN 47906, USA
hsuh@purdue.edu, dperouli@purdue.edu

Abstract—In this paper, the viscoelastic behavior of a tunable RF-MEMS resonator and its impacts are studied by means of direct RF measurements for the first time. This tunable resonator consists of one $\lambda/2$ coplanar waveguide (CPW) resonator and two nanocrystalline-Ni RF-MEMS varactors. S-parameters of this tunable resonator have been measured for 80 hours under a bi-state bias condition of 0 and 40 V. It is demonstrated that the resonant frequency is shifted by 90 MHz and the varactor deformed by $0.12 \mu\text{m}$ over the 80 hour period. The gap of the loaded varactor is extracted from the measured S-parameters using finite-element analysis (FEA) tools. A generalized Voigt-Kelvin model is employed to verify the viscoelastic behavior of the resonator. The creep compliance extracted from the RF measurements is in excellent agreement with results in literature.

Index Terms—creep, nickel, RF-MEMS, tunable resonator, viscoelastic.

I. INTRODUCTION

Planar tunable RF-MEMS filters are critical components in reconfigurable RF front-ends. Several such RF-MEMS filters with attractive features including small size, low power, and high linearity have already been demonstrated [1]–[5]. The classic architecture includes a medium to high-Q planar resonator and digital or analog tunable capacitors (varactors). Due to the need for obtaining high-Q varactors, highly conductive thin-films such as Au, Al, and Ni are commonly employed in these varactors. Although not completely understood, the viscoelastic behavior of these materials [6]–[10] may adversely impact the long-term operation of RF MEMS filters. This may be seen as a drift of the resonant frequency and/or tuning range of the filter, reduction of the pull-in voltage, and decrease of the restoring force in the varactors.

Vicker-Kirby *et al.* reported anelastic phenomena in MEMS cantilever accelerometers made of Si, Ni, and Au [6] for 30 hours. This experiment demonstrated that Au is prone to creep most among the three materials. Gilz *et al.* performed an experiment on an Al RF-MEMS switch for 15 hours [7]. This switch was pulled-in using electrostatic force and the deformation of the suspension beam was measured optically. Yan *et al.* performed a stress-relaxation test on an Au thin-film using a bulge test technique for 80 hours [8]. A cyclic-loading test was also carried out to demonstrate the linearity of viscoelasticity in such films. It showed that the restoring force of an RF-MEMES switch might decrease by 20 % after

operation of 72 hours. The authors developed an ultra low-noise experimental techniques to characterize the viscoelastic behavior of Ni-based MEMS structures up to 1,370 hours [9], [10].

The studies above provide insights into potential failure modes in RF-MEMS filters. However, to the authors' best knowledge, viscoelastic behavior of tunable RF-MEMS filters/resonator has not been directly characterized by means of RF measurements. In this work, for the first time, the long-term S-parameters of a planar resonator tuned by RF-MEMS varactors are reported for over 80 hours. A bi-state bias condition is adopted to reveal the time-dependent resonant frequency and tuning-range of the resonator. The gap change of the RF-MEMS varactor is extracted from the measured S-parameters and used in a generalized Voigt-Kelvin model. The creep compliance extracted from the RF measurements using this model is consistent with the literature [10].

II. DESIGN AND FABRICATION

The tunable RF-MEMS resonator under study is shown in Fig. 1. This resonator consists of a $50\text{-}\Omega$ coplanar-waveguide (CPW) resonator and two analog RF-MEMS varactors symmetrically loaded at both ends of the resonator. The bias voltage is applied on the center conductor of the CPW resonator via a highly-resistive SiCr bias-line. The moving plate of the varactor is $200\text{-}\mu\text{m}$ long and $120\text{-}\mu\text{m}$ wide. The length and width of the suspension beam are $200 \mu\text{m}$ and $20 \mu\text{m}$ respectively. The thickness of the Ni varactor is $3 \mu\text{m}$ and the actuation voltage is about 75 V. The anchor of the varactor is designed to enhance adhesion. The resonator is weakly coupled to the feed-line and ground-signal-ground pads with an open-section of $30 \mu\text{m}$. The calculated spring constant of the varactor is 51 N/m [10]. According to the equivalent circuit of this tunable resonator in Fig. 2, the resonant frequency is a function of the capacitance and position of the loaded varactor [1]. It is implicitly given by

$$\overline{B}_p - \cot\theta_2 + \tan\theta_1 = 0 \quad (1)$$

where θ_1 and θ_2 are the equivalent electrical lengths of l_1 and l_2 , and \overline{B}_p is the normalized total shunt susceptance, which is mainly contributed by the varactors. In this paper, l_1 and l_2 are $150 \mu\text{m}$ and $485 \mu\text{m}$ respectively. The initial C_{var} extracted using finite-element-analysis (FEA) is 60 fF [11].

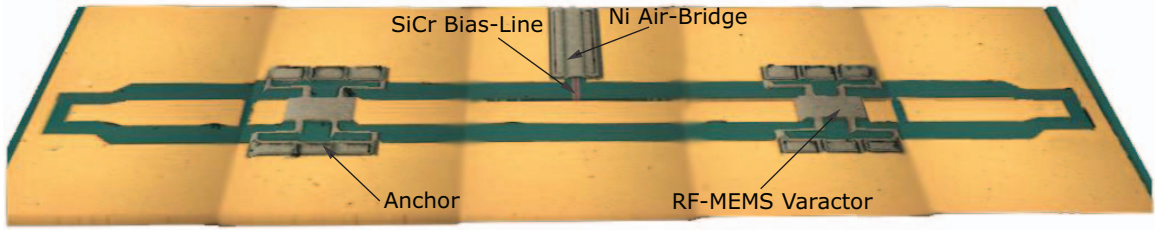


Fig. 1. The confocal-microscopy image of the tunable RF-MEMS resonator. The resonator consists of an $1,270\text{-}\mu\text{m}$ long CPW resonator and two analog RF-MEMS varactors. This picture is made by tiling 10 images from the confocal microscope.

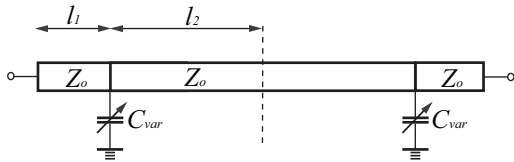


Fig. 2. Schematic of the tunable resonator loaded with two RF-MEMS varactors.

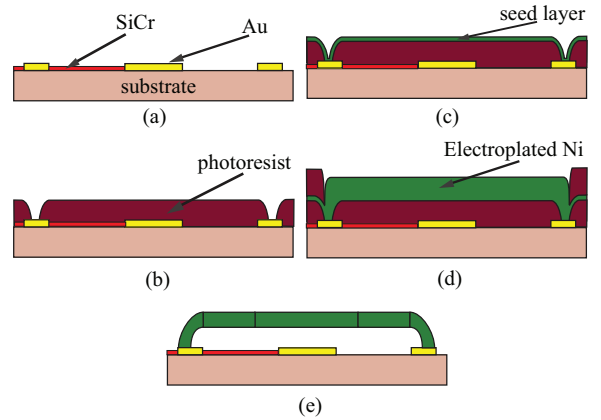


Fig. 3. Fabrication process of the tunable RF-MEMS resonator.

The fabrication process of this tunable RF-MEMS resonator is shown in Fig. 3. The varactor is built on a p -type high-resistivity silicon substrate with a 500-nm thick thermally-grown silicon-dioxide film. A 100-nm thick SiCr-film and an $1\text{-}\mu\text{m}$ thick Au-film are sputtered and lifted-off to define the CPW and electrical connections of the resonator (Fig. 3(a)). The anchors are then patterned through a $3\text{-}\mu\text{m}$ thick photoresist sacrificial layer (Fig. 3(b)). The sacrificial layer is hard-baked at 190°C for 5 minutes for two reasons. First, hard-baking removes the residual solvent in the photoresist and prevents it from outgassing. Second, better corner-coverage of the seed layer can be obtained by rounding the sharp corners of the photoresist with hard-baking. A seed-layer of 50-nm sputtered Ti and 30-nm evaporated Ni is deposited on the whole sample (Fig. 3(c)). A $6\text{-}\mu\text{m}$ thick photoresist layer is shaped to form the electroplating mold on the seed layer. The Ni electroplating is carried out in a nickel-sulfamate bath at a temperature of 50°C and a pH value of 4. The average grain-size is about 50 nm . A $3\text{-}\mu\text{m}$ thick Ni layer is electroplated on the seed layer selectively based on the photoresist mold (Fig. 3(d)). The Ni and Ti seed layer are stripped with $\text{HCl} : \text{water} = 1 : 1$ and $\text{HF} : \text{water} = 1 : 20$ at room temperature respectively after the removal of the photoresist mold. The photoresist sacrificial layer is removed by immersion in photoresist-stripper-2000 at 75°C for 24 hours. Finally, the fabrication process is completed by drying in a critical-point-dryer (Fig. 3(e)). According to the confocal-microscope measurement, the initial gap of the varactor is approximately $4.3\text{ }\mu\text{m}$ instead of the nominal value $3\text{ }\mu\text{m}$ because of the compressive residual-stress in the Ni layer.

III. RESULTS AND DISCUSSION

A. Measured Data

The RF measurements are conducted with the Agilent PNA E8361C network analyzer. The measurement setup is cali-

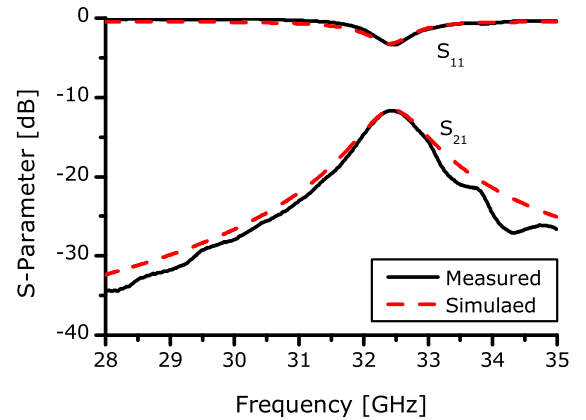


Fig. 4. The measured and simulated S-parameters of the tunable RF-MEMS resonator at $t = 0$ and $V_{bias} = 0$.

brated with an on-wafer TRL calibration kit. The measured S-parameters of the tunable resonator at $t = 0$ and $V_{bias} = 0$ are compared with the FEA simulation and show good consistency in Fig. 4 [12]. The conductivity and relative permeability of Ni at K-band are $7.9 \times 10^6\text{ S}$ and 1.7 respectively. These are experimentally-extracted in [13]. It's worth noting that the high-frequency permeability of Ni is required in order to obtain an accurate simulation.

The tunable RF-MEMS resonator is measured using a bi-state bias condition. In the first state a constant bias-voltage

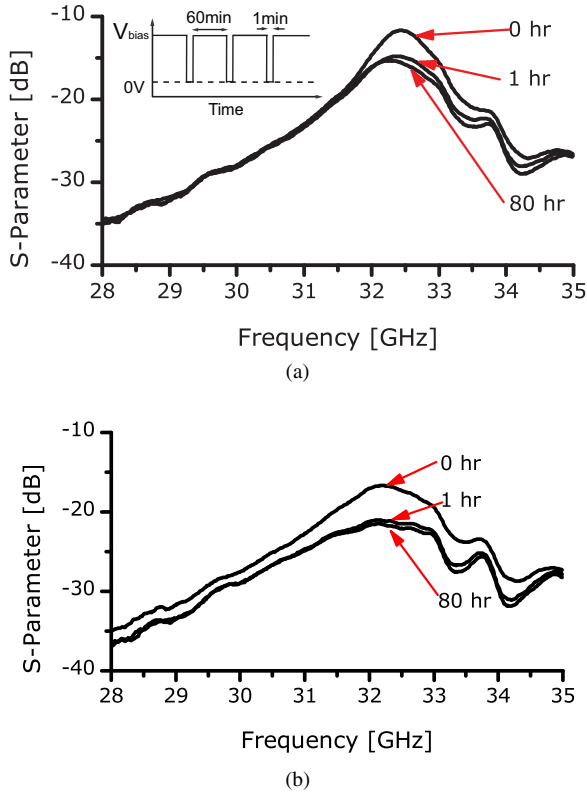


Fig. 5. The measured S_{21} of the tunable RF-MEMS resonator at 0, 1, and 80 hours. (a) Unbiased ($V_{bias} = 0$). (b) Biased ($V_{bias} = 40V$).

V_{bias} is applied to the varactor for 60 minutes. In the second state the bias voltage is removed for 1 minute. This is a variation of the constant-voltage bias condition that can be found in many RF-MEMS applications. This variation provides insight into the tuning range and dynamics of the tunable RF-MEMS devices. In Fig. 5 the biased curves represent the S_{21} measured in the first bias state when V_{bias} is 40 V. The S_{21} measured in the second state when V_{bias} is removed is shown in the unbiased curves. The resonant frequencies at both biased and unbiased states are obtained from the measured S-parameters and are depicted in Fig. 6. The initial frequency before any bias is applied is shown as f_o .

This time-dependent resonant frequency can be modeled using a series of decaying exponents,

$$f(t) = A_o + \sum_{i=1}^n A_i e^{-t/\tau_i} \quad (2)$$

where A_i and τ_i are constants as shown in Table I. Two regions can be identified in Fig. 6. In the first 3 hours, the frequency decreases rapidly with an increasing slope. In the second region, the slope of the frequency approximates a constant value after about 3 hours. Because of the viscoelastic behavior of the two RF-MEMS varactor, the resonant frequency can not revert to the initial frequency f_o and is determined by the loading history. The frequency shift is up to 90 MHz which occurs at the 80th hour and 0 V. This imposes two challenges to tunable RF-MEMS filters. First, the filter may drift away

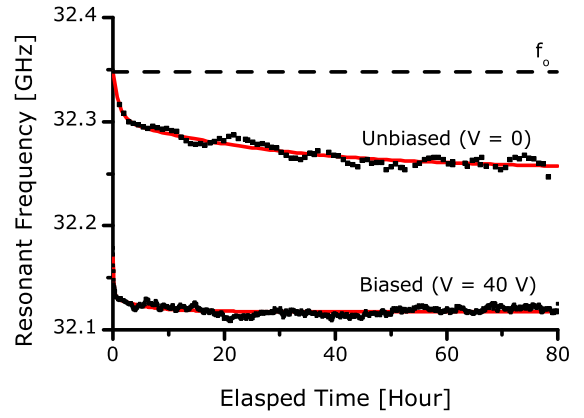


Fig. 6. The measured (black) and fitted (red) resonant-frequency of the tunable RF-MEMS resonator over 80 hours. f_o is the initial resonant-frequency.

TABLE I
FITTING PARAMETERS OF RESONANT FREQUENCY

| | A_0^* | A_1 | τ_1^* | A_2 | τ_2 |
|-----------------------|---------|--------|------------|--------|----------|
| Unbiased ($V = 0$ V) | 32.254 | 0.0463 | 1.135 | 0.0478 | 30.644 |
| Biased ($V = 40$ V) | 32.117 | 0.0142 | 5.500 | 0.0389 | 0.184 |

* A_i is in GHz and τ_i is in hours.

from the desired frequency even though the designed voltage is applied. Second, the filter may not be able to cover the desired band after a long-period of operation. For a bias voltage of 0–40 V, the resonator tunes from 32.17–32.35 GHz at $t = 0$. The range shifts to 32.11–32.26 GHz after operation of 80 hours. The change of the resonant frequency is expected to be even greater if the full tuning range of the varactors (0–75 V) is used.

B. Extraction of Creep Compliance

The creep compliance is the critical parameter to characterize a linear viscoelastic system and is defined as [14]

$$D(t) = \frac{\epsilon(t)}{\sigma_o} \quad (3)$$

where $\epsilon(t)$ is the strain as a function of time and σ_o is the applied constant stress. The creep compliance can be extracted from the RF measurements and compared to the results obtained using other experimental methods [10]. This will validate the results obtained from this method. In order to obtain the extracted creep compliance, the parameters of the generalized Voigt-Kelvin model are required. It is a widely-used model to describe the creep compliance of linear viscoelastic systems with multiple time constants,

$$D(t) = \left[\frac{1}{E_o} + \sum_{i=1}^n \frac{1}{E_i} \left(1 - e^{-t/\tau_i} \right) \right] \quad (4)$$

where τ_i is time constant and E_i is elastic modulus.

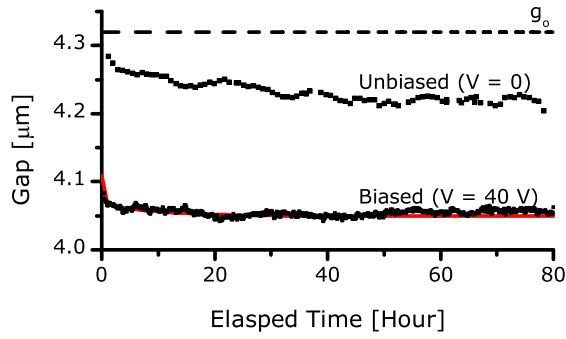


Fig. 7. The FEA-extracted gap (black) of the loaded varactor. The generalized Voigt-Kelvin model is shown in red. The parameter g_0 is the initial gap before any bias is applied.

First, the gap and the electrostatic force of the varactor need to be extracted from the measured S-parameters using FEA tools as shown Fig. 7 (gap only). The parasitics and fringing fields are included in the FEA extraction. Second, a hypothetical gap is calculated using Boltzmann superposition principle based on (4),

$$\delta(t) = \frac{E}{K} \left[F(0)D(t) + \int_{0+}^t D(t-\xi) \frac{dF(\xi)}{d\xi} d\xi \right] \quad (5)$$

where E is the Young's modulus, K is the spring constant, and $F(t)$ is the electrostatic force. Third, the parameters E_i and τ_i in (4) are adjusted until this hypothetical gap coincides with the FEA-extracted gap. A least-square fit and the Levenberg-Marquardt algorithm are utilized in the adjustment [15]. Finally, the parameters of the creep compliance that match the extracted gap are listed in Table II.

The gap calculated using the generalized Voigt-Kelvin model matches the extracted gap very well. It is observed that the gap shifts up to $0.12 \mu\text{m}$. The discrepancy in Fig. 8 may be introduced by the compressive residual-stress in the electroplated Ni film. In spite of the slight difference in time constant, the creep-compliance extracted from RF measurement and other methods show very good agreement.

IV. CONCLUSION

The viscoelastic behavior of a tunable RF-MEMS resonator has been characterized using direct RF measurements. The evolution of S-parameters, resonant frequency, and tuning range under a bi-state bias condition over 80 hours are presented. The gap of the loading varactor is extracted using a FEA tool. The resonant frequency and the varactor gap shifted by 90 MHz and $0.12 \mu\text{m}$ respectively. The creep compliance extracted from the RF measurement is consistent with the results obtained using other experimental methods. The effectiveness of RF measurements on viscoelasticity in RF-MEMS devices is demonstrated.

ACKNOWLEDGEMENT

This material is based upon work supported by NNSA Center of Prediction of Reliability, Integrity, and Survivability

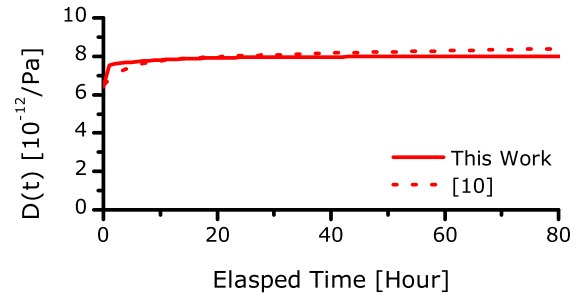


Fig. 8. The comparison of extracted creep-compliance. The creep compliance extracted from the S-parameter shows good consistency with the literature.

TABLE II
FITTING PARAMETERS OF CREEP COMPLIANCE

| E_0^* | E_1 | τ_1^* | E_2 | τ_2 |
|---------|---------|------------|---------|----------|
| 156.109 | 902.582 | 0.309 | 2145.04 | 10.245 |

* E_i is in GPa and τ_i is in hours.

of Microsystems, and Department of Energy under Award Number DE-FC52-08NA28617.

REFERENCES

- [1] A. Abbaspour-Tamijani, L. Dussopt, and G. M. Rebeiz, "A millimeter-wave tunable filter using mems varactor," in *IEEE MTT-S Int. Microwave Symp. Dig.*, June 2003, pp. 1785–1788.
- [2] —, "Miniature and tunable filters using mems capacitors," *IEEE Trans. Microwave Theory Tech.*, July 2003.
- [3] E. Fourn, A. Pothier, C. Champeaux, P. Tristant, A. Catherinot, P. Blondy, C. P. Grard Tann, Eric Rius, and F. Huret, "Mems switchable interdigital coplanar filter," *IEEE Trans. Microwave Theory Tech.*, Jan. 2003.
- [4] K. Entesari and G. M. Rebeiz, "A 1218-ghz three-pole rf mems tunable filter," *IEEE Trans. Microwave Theory Tech.*, vol. 53, no. 8, pp. 2566–2571, Aug. 2004.
- [5] B. Pillans, A. Malczewski, R. Allison, and J. Brank, "6–15 ghz rf mems tunable filters," in *IEEE MTT-S Int. Microwave Symp. Dig.*, June 2005.
- [6] D. J. Vickers-Kirby, R. L. Kubena, F. P. Stratton, R. J. Joyce, D. T. Chang, and J. Kim, "Anelastic creep phenomena in thin metal plated cantilevers for mems," in *Mat. Res. Soc. Symp.*, vol. 657, 2001, pp. EE2.5.1–EE2.5.6.
- [7] M. van Gils, J. Bielen, and G. McDonald, "Evaluation of creep in rf mems devices," in *EuroSime*, Apr. 2007, pp. 1–6.
- [8] X. Yan, W. L. Brown, Y. Li, J. Papapolymerou, C. Palego, J. C. M. Hwang, and R. P. Vinci, "Anelastic stress relaxation in gold films and its impact on restoring forces in mems devices," *J. Microelectromech. Syst.*, vol. 18, no. 3, pp. 570–576, June 2009.
- [9] H.-H. Hsu and D. Peroulis, "A viscoelastic-aware experimentally-derived model for analog rf mems varactors," in *IEEE International Conference on Micro Electro Mechanical Systems*, Jan. 2010, pp. 783–786.
- [10] —, "Viscoelastic behavior in nanocrystalline nickel rf-mems based on analog varactors," *J. Microelectromech. Syst.*, under preparation.
- [11] Ansoft maxwell 3d. Ansoft LCC. Version 12, 2008. [Online]. Available: <http://www.ansoft.com>
- [12] Ansoft hfss. Ansoft LCC. Version 10, 2008. [Online]. Available: <http://www.ansoft.com>
- [13] H.-H. Hsu, S. W. Lee, and D. Peroulis, "K-band loss characterization of electroplated nickel for rf mems devices," in *IEEE Antennas and Propagation International Symposium*, June 2007.
- [14] H. F. Brinson and L. C. Brinson, *Polymer Engineering Science and Viscoelasticity An Introduction*. New York: Springer, 2008.
- [15] Mathematica. Wolfram Research. Version 6, 2007. [Online]. Available: <http://www.wolfram.com>